A Symbolic Sensitivity Method for Mismatch Analysis and CMRR Improvement

Shuwen Deng*, Hanbin Hu† and Guoyong Shi‡
Dept of Micro/Nano-electronics, Shanghai Jiao Tong University, Shanghai 200240, China
Email: *swdeng.betty@outlook.com, †hanbinhu2016@gmail.com, ‡shiguoyong@sjtu.edu.cn

***Abstract*—Mismatch and Common Mode Rejection Ratio (CMRR) are becoming a concern in biopotential signal processing circuits in the application of weak signal acquisition using low-power and low-voltage design techniques. Proper tools are needed to quickly locate the sensitive mismatch components to improve the matching quality and CMRR. This paper proposes a symbolic sensitivity based technique that can help quickly localize the mismatch-sensitive components and suggest intuitive guide for resizing. Example is given to justify the validity of the proposed method.**

***Index Terms*—Mismatch, common mode rejection ratio (CMRR), Monte Carlo analysis, symbolic sensitivity.**

I. Introduction

Common mode rejection ratio (CMRR) is a measure of an operational amplifier's (opamp's) capability in rejecting common-mode signal in differential operation. A differential opamp has two inputs, which could carry a common level of input signal. Denoting by v_d and v_{cm} the differential- and common-mode signal components, we may write the respective output voltages from the opamp by $v_{out}^d = A_v v_d$ and $v_{out}^{cm} = A_{cm} v_{cm}$, where A_v and A_{cm} are the differential- and common-mode voltage gains, respectively. Then CMRR is defined as (referring to Fig. 1) [1]

$$\mathrm{CMRR} = \left| \frac{A_v}{A_{cm}} \right|, \tag{1}$$

i.e., the ratio between the differential-mode gain and the common-mode gain.

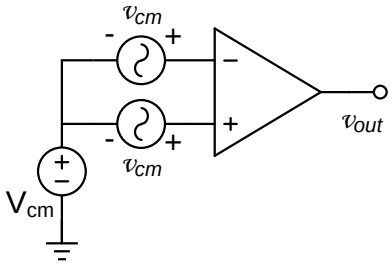

Fig. 1. Measurement of CMRR.

Recently there have appeared a number of works studying the design techniques for improving biopotential signal acquisition capability of low-voltage/low-power circuits, among them CMRR enhancement techniques are of special interest [2]–[6]. Due to the weak fluctuation of biomedical instrumentation, common-mode noise is one of the most critical issues in biomedical circuit design. Facing the increasing uncertainty in analog circuit design and decreasing supply voltage, advanced circuit design techniques are needed to achieve a better CMRR target.

Several circuit design techniques are proposed in the literature for improving CMRR performance, such as leveraging trimming, auto-zeroing, and chopping. However, these techniques have limited capability in capturing the most sensitive circuit element pertinent to CMRR. CMRR-sensitive elements require more attention during layout design.

Since CMRR is measured from small signal excitations, its analytical property with respect to circuit element can be deduced by symbolic analysis. Recently, the application of the notion of *symbolic sensitivity* has been explored in several papers [7], [8]. It is advantageous in quickly identifying the most sensitive circuit elements regarding the selected design metrics. It has also been demonstrated that *symbolic sensitivity* is an intuitive approach to CMOS circuit sizing.

In this paper we apply the same technique for improving CMRR property of opamp concerning the mismatch of the externally connected peripheral circuit elements. We found in experiment that symbolic sensitivity analysis could quickly identify the most CMRR-sensitive element and its reference value; with this information designer would pay special attention to such elements during layout design.

The basic principle for symbolic computation of CMRR and its sensitivity is introduced in section II. A design example is analyzed by using the proposed method for CMRR optimization, and the efficiency is compared to the Monte Carlo method in Section III. Section IV concludes the paper.

II. Symbolic CMRR Calculation and Sensitivity

The calculation of CMRR involves two input-output (I/O) pairs: 1) From the differential signal input to the opamp output with the gain A_v and 2) from the common-mode perturbation to the opamp output with the gain A_{cm}. Both gains are small-signal gains and are computable by running AC analysis with a Spice simulator. But Spice simulation does not provide analytical information. Obtaining analytical dependence on the circuit parameters must resort to a symbolic circuit simulator [9]. Since symbolic sensitivity computation is an involved procedure, a particular mechanism for symbol representation and manipulation can make great difference in computational

[1]This research was sponsored by the National Natural Science Foundation of China (NSFC) under the grant No. 61176129 and No. 61474145.

efficiency. The work [10] has made comparison on this issue and justified that the GPDD (Graph-Pair Decision Diagram) symbolic method [11] is most suitable for such computation.

As an illustration of the basic principle, let us take a look at the example shown in Fig. 2, where a Binary Decision Diagram (BDD) on the right-hand side is a symbolic representation of the I/O relation of the circuit beside. This BDD (with a particular name GPDD reflecting its underlying algorithm) can be constructed and saved in the computer memory with excellent efficiency. The book [9] explains all the technical details regarding the GPDD algorithm.

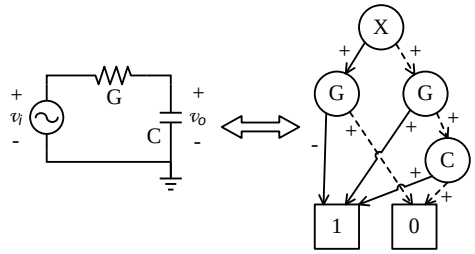

Fig. 2. GPDD example.

The GPDD algorithm can easily deal with multiple inputs and outputs as well. In its application to the symbolic computation of CMRR we only need to consider two inputs and one single output for the computation of the two gains A_v and A_{cm} that share the common output. Since both gains are computed on the same circuit, the symbolic representations for A_v and A_{cm} can share one GPDD in the computer memory, which is a computational advantage by using GPDD.

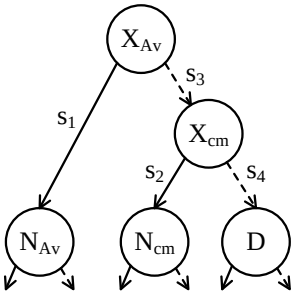

Fig. 3. GPDD for CMRR analysis, where s_k's stand for the directed edge signs.

Both I/O ports involved in CMRR belong to voltage controlled voltage sources (VCVS) ports, whose transfer functions are denoted by X_{Av}^{-1} and X_{cm}^{-1} (note that GPDD construction requires port inversion), where X_{Av} and X_{cm} are two symbols in the shared GPDD. By construction, they are placed closest to the root as illustrated in Fig. 3. The vertices N_{Av}, N_{cm} and D in the diagram have offspring vertices not shown in the figure. We denote by $f(V)$ the symbolic function represented by the sub-diagram pointed by a generic vertex V. Then the two gains involved in CMRR computation can be calculated symbolically as follows:

$$A_v = \frac{1}{X_{Av}} = -s_1 s_3 s_4 \frac{f(N_{Av})}{f(D)} \quad (2)$$

$$A_{cm} = \frac{1}{X_{cm}} = -s_2 s_4 \frac{f(N_{cm})}{f(D))} \quad (3)$$

where the s_k's are the diagram edge signs [9].

By the CMRR definition (1), it then holds that

$$\mathrm{CMRR} = s_1 s_2 s_3 \frac{f(N_{Av})}{f(N_{cm})}. \quad (4)$$

So far we have gone through the computation flow of obtaining a symbolic representation of CMRR. We emphasize the a symbolic CMRR is a Binary Decision Diagram with vertices representing the circuit symbols. Any symbol is traceable by traversing the diagram from the root. Another important property is that no vertex in the diagram involves composite symbol (i.e., arithmetic expression of basic symbols). This property is particularly meaningful for sensitivity computation.

Sensitivity is a good measure for pinpointing those few parameters that are worth most attention in the circuit physical design stage. When it is applied to CMRR, we are interested in the effect of mismatch on the CMRR metric.

The sensitivity of a transfer function $H(s)$ with respect to an arbitrary parameter p is typically defined by the following normalized form:

$$Sens(H(s), p) := \lim_{\Delta p \to \infty} \left\{ \frac{\frac{\Delta H(s)}{H(s)}}{\frac{\Delta p}{p}} \right\} = \frac{p}{H(s)} \frac{\partial H(s)}{\partial p} \quad (5)$$

The symbolic expression in GPDD is composed of sum-of-products with each product term containing basic circuit parameters. As a result, taking derivative as the expression $\frac{\partial H(s)}{\partial p}$ is extremely simple as explained in detail in [10].

Noting that CMRR is the ratio of two transfer functions, we can readily verify that

$$Sens(\mathrm{CMRR}, p) = Sens(|A_v|, p) - Sens(|A_{cm}|, p) \quad (6)$$

Therefore, as long as the sensitivities of the two transfer functions $A_v(s)$ and $A_{cm}(s)$ with respect to p are known, the CMRR sensitivity is obtained directly.

III. Experimental Results

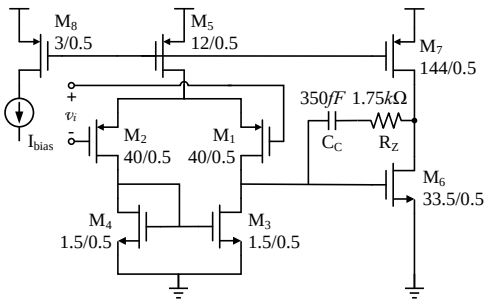

Fig. 4. Two-stage opamp with Miller compensation.

The proposed computation method for CMRR and its sensitivity has been implemented in the GPDD software prototyping

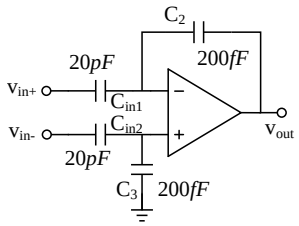

Fig. 5. Opamp with external capacitors.

system written in C++ in the authors' laboratory. HSPICE simulation results were used for comparison. Shown in Fig. 4 is a two-stage opamp sized with the TSMC 0.18μm CMOS technology. We assume that four peripheral capacitors are connected to the opamp in a typical application as shown in Fig. 5. Fig. 6 shows a good agreement of the CMRR versus frequency (up to 100MHz) computed by GPDD and HSPICE.

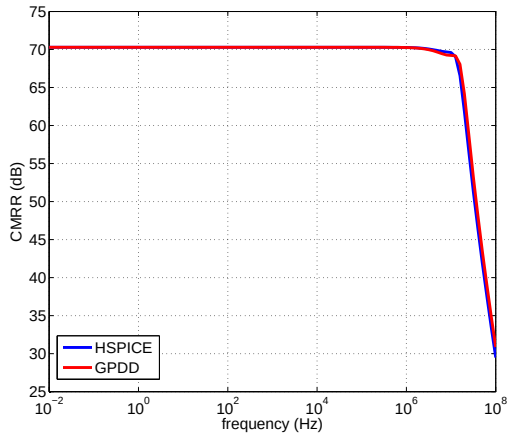

Fig. 6. CMRR results of the two-stage opamp.

A. Optimization by CMRR Sensitivity

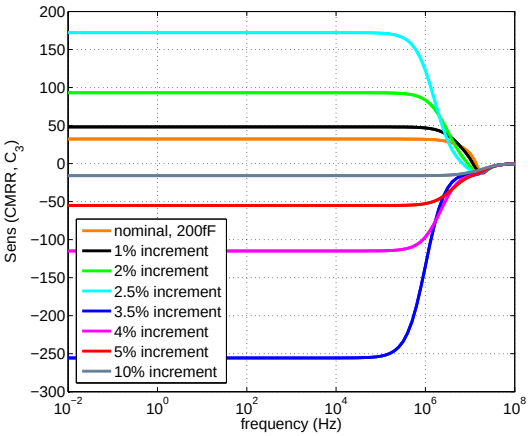

Fig. 7. Evolutional sensitivity with respect to the variation of C_3.

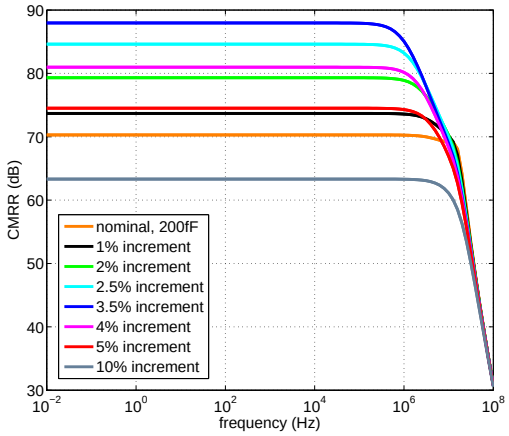

Fig. 8. Evolutional CMRR with respect to the variation of C_3.

The recent paper [6] discussed impedance matching for biopotential signal acquisition. That method did not consider the influence of the opamp internal impedance (like R_z and C_c in the compensation path connected to the opamp output) on the determination of the mismatch factor between the pair of capacitors C_2 and C_3. The exact matching of them does not mean the best CMRR unless in the situation of an ideal opamp. By sizing the pair of C_2 and C_3 identical with the value 200 fF, the opamp only achieves a CMRR of nearly 70.29dB, which is not satisfactory yet.

Hence, in the experiment we report mainly a search of a proper C_3 independent of C_2 to come up with a optimized CMRR. Although sweeping of C_3 fulfils the role, here we examine the advantage of guiding the search by symbolic sensitivity. We show by evolutional running to reveal how the sensitivity helps us reduce the blindness in the search.

We computed a bundle of sensitivity curves of CMRR by increasing C_3 with a grid of percentages. As seen from Fig. 7, the sensitivity curves exhibit an interesting phenomenon. As C_3 is increased from its nominal $200fF$, the level part of the sensitivity curve starts to rise but remains positive. At the grid of 2.5% it reaches the topmost; as we further increase C_3 to 3.5% it flips over to the bottommost negative sensitivity. We did another run at the grid of 3.0% to get a nearly optimum CMRR at $100.5dB$. The evolutional numbers are recorded in Table I where the row with underscore corresponds to the optimized result.

Remark 1: Computing numerical sensitivity of CMRR by HSPICE is also possible, but would require two runs for each parameter value followed by relative difference calculation. Comparatively, symbolic CMRR sensitivity computation by GPDD is analytical and 100% accurate except for numerical roundoff errors.

B. Comparison to Monte Carlo

Mismatch also can be examined by Monte Carlo simulation, but it is more time-consuming and lacks insight. For example,

TABLE I
CMRR OPTIMIZATION PROCESS

Increment of C3	$Sens\,(\mathrm{CMRR}, C_3)$	CMRR (dB)
0	32.313	70.3
1%	48.211	73.7
2%	93.1415	79.3
2.5%	172.226	84.6
3%	1.082K	100.5
3.5%	-255.656	88.0
4%	-114.933	81.0
4.5%	-74.381	77.2
5%	-55.118	74.5
6%	-36.486	70.8
10%	-15.925	63.3

we may check the random mismatch between the input capacitor pair C_{in1} and C_{in2} and the other capacitor pair C_2 and C_3 by Monte Carlo sampling. The Monte Carlo simulation result shown in Fig. 9 shows the normalized histogram of 1,000 samples for the CMRR measure with respect to one of the four capacitors. It took nearly 547.031 milliseconds by HSPICE to calculate 1,000 samples at $f = 50Hz$ for each circuit component with 0.2% mismatch. Table II shows more statistical details. As a comparison, the sensitivity computation using GPDD took only 3.001 milliseconds on average. We observe that the sensitivity results correlate very well with the Monte Carlo variance. There is no doubt that sensitivity analysis is a much faster way for mismatch effect examination.

The Monte Carlo result shows that the mismatch of the input pair of capacitors C_{in1} and C_{in2} affects more on the CMRR performance, calling for more attention during layout design. This is confirmed by the sensitivity result computed by GPDD as well, see Fig. 10.

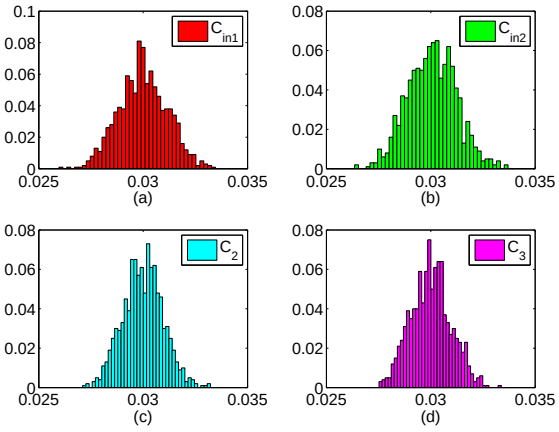

Fig. 9. Monte Carlo results of $|A_{cm}(s)|$ at $f = 50Hz$ with 1,000 runs.

IV. CONCLUSION

This article presents a symbolic sensitivity approach to CMRR optimization over capacitive mismatch. This work is motivated by the rising needs in opamp design for biopotential signal acquisition. The proposed technique is expected to be applicable to other areas of sensor node circuit design

TABLE II
COMPARISON OF PARAMETER VARIATION BY RUNNING MONTE CARLO ANALYSIS AND SENSITIVITY AT 50HZ WITH 0.2% ELEMENT MISMATCH.

Element	Mean	Std. Var	$\lvert Sens\,(A_{cm})\rvert$
C_{in1}	30.02m	1.298μ	37.30
C_{in2}	29.98m	1.415μ	38.23
C_2	30.01m	0.887μ	31.33
C_3	30.01m	0.900μ	32.31

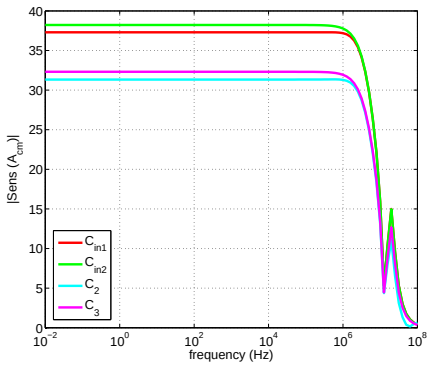

Fig. 10. Common mode gain sensitivity computed by GPDD.

where signals are weak and power supplies are limited and noisy. Future work will pay more attention to the automatic optimization issue based on the notion of symbolic sensitivity.

REFERENCES

[1] P. R. Gray, P. J. Hurst, S. H. Lewis, and R. G. Meyer, *Analysis and Design of Analog Integrated Circuits*, 4th ed. Singapore: John Wiley & Sons, Inc., 2001.

[2] A. Harb and M. Sawan, "New low-power low-voltage high-CMRR CMOS instrumentation amplifier," in *Proc. IEEE Int'l Symposium on Circuits and Systems (ISCAS)*, vol. 6, July 1999, pp. 97–100.

[3] R. R. Harrison and C. Charles, "A low-power low-noise CMOS amplifier for neural recording applications," *IEEE J. Solid-State Circuits*, vol. 38, no. 6, pp. 958–965, June 2003.

[4] V. Ivanov, J. Zhou, and I. M. Filanovsky, "A 100-dB CMRR CMOS operational amplifier with single-supply capability," *IEEE Trans. on Circuits and Systems II: Express Briefs*, vol. 54, no. 5, pp. 397–401, May 2007.

[5] M. A. P. Pertijs and W. J. Kindt, "A 140 dB-CMRR current-feedback instrumentation amplifier employing ping-pong auto-zeroing and chopping," *IEEE J. Solid-State Circuits*, vol. 45, no. 10, pp. 2044–2056, Oct 2010.

[6] R. Abdullah and E. Sánchez-Sinencio, "A biopotential amplifier with dynamic capacitor matching for improved CMRR," *Analog Integrated Circuits and Signal Processing*, vol. 82, no. 1, pp. 47–55, January 2015.

[7] G. Shi and X. Meng, "Variational analog integrated circuit design by symbolic sensitivity analysis," in *Proc. Int'l Symposium on Circuits and Systems (ISCAS)*, Taiwan, China, May 2009, pp. 3002–3005.

[8] G. Shi, J. Chen, A. Tai, and F. Lee, "A size sensitivity method for interactive CMOS circuit sizing," *Analog Integrated Circuits and Signal Processing*, vol. 77, no. 2, pp. 96–104, 2013.

[9] G. Shi, S. X.-D. Tan, and E. Tlelo-Cuautle, *Advanced Symbolic Analysis for VLSI Systems – Methods and Applications*. New York: Springer, 2014.

[10] G. Shi, "A survey on binary decision diagram approaches to symbolic analysis of analog integrated circuits," *Analog Integrated Circuits and Signal Processing*, vol. 74, no. 2, pp. 331–343, 2013.

[11] ——, "Graph-pair decision diagram construction for topological symbolic circuit analysis," *IEEE Trans. on Computer-Aided Design of Integrated Circuits and Systems*, vol. 32, no. 2, pp. 275–288, February 2013.